Since January 2020 Elsevier has created a COVID-19 resource centre with free information in English and Mandarin on the novel coronavirus COVID-19. The COVID-19 resource centre is hosted on Elsevier Connect, the company's public news and information website.

CHAPTER 2

Nanomaterial-Based Photocatalysis

2.1 INTRODUCTION

Since the last few decades, nanostructured materials (NsM) have been explored and investigated curiously worldwide in various applications including energy and environmental. NsM could be defined as the solids composed of structural elements—mostly crystallites—with a characteristic size (in at least one direction) of a few nanometers (1−100 nm). These materials exhibit outstanding and often superior physical and chemical properties compared with their bulk counterpart because of different chemical composition, arrangement of the atoms, and size. The growth of NsM in one, two, and three dimensions generates new interesting properties, which remarkably enhanced functions for device fabrication in various fields, including energy, medical, biological, opto-electronics, optics, magnetic, electronic, and many others. Particularly, metal and metal oxide nanostructures have been studied potentially due to their high specific surface to volume ratio, showed quantum size effect, properties can be controlled just adjusting shape and size and high interfacial reactivity. NsM could be classified into four types—zero: clusters of any aspect ratio from 1 to ∞; one: multilayers; two: ultrafine-grained overlayers or buried layers; and three: nanophase materials depend on their dimensional grain growth (Figure 2.1). The properties of NsM are examined by their size distribution, shape, chemical composition and interfacial reactivity, and type of grains present at the interfaces [1]. The change in the size makes these materials have different electronic changes in terms of energy and number of levels. This makes these materials behave electronically different. The origin of the size-induced properties in nanomaterials depends basically on the surface phenomena (extrinsic contribution) and quantum confinement effects (intrinsic contribution). This chapter gives a detailed summary about NsM and their outstanding properties [2].

Heterogeneous Nanocomposite-Photocatalysis for Water Purification.

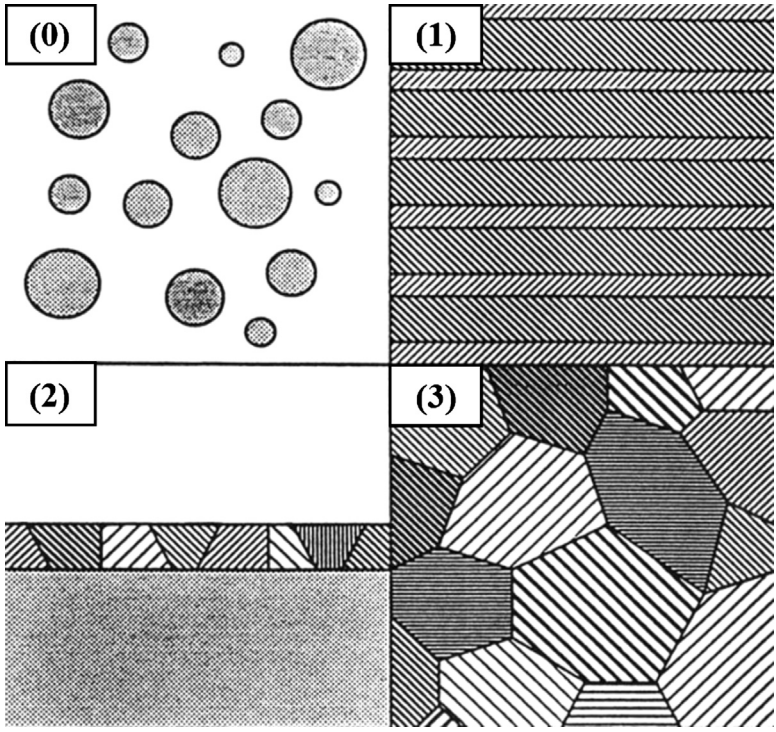

Figure 2.1 Schematic of the four types of nanostructured materials. Reproduced from Ref. 1.

2.2 PROPERTIES OF NsM

2.2.1 Increase in Surface Area to Volume Ratio

First, nanomaterials have a relatively larger surface area compared with the same volume (or mass) of the material produces in a larger form. Let us consider a sphere of radius "*r*," surface area, and volume of sphere given in Eqs. (2.1) and (2.2). The ratio of these two equations gives Eq. (2.3), which indicates the increase in surface to volume ratio with decrease in size of materials. Thus, when the radius of the sphere decreases, its surface area to volume ratio increases [3,4]. Figure 2.2 shows the relation between surface area and size of silica nanoparticles. It is seen that obtained surface area increased exponentially below 100 nm indicated crucial role of size in NsM. If a bulk material is subdivided into an ensemble of individual nanomaterials, the total volume remains the same, but the collective surface area is greatly increased.

$$\text{Its surface area } A = 4\pi r^2 \tag{2.1}$$

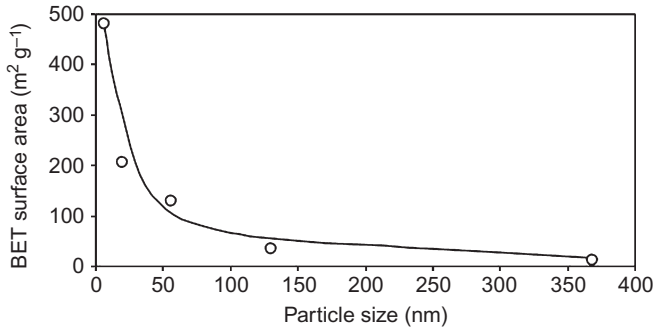

Figure 2.2 Effect of size on surface area of silica nanoparticles.

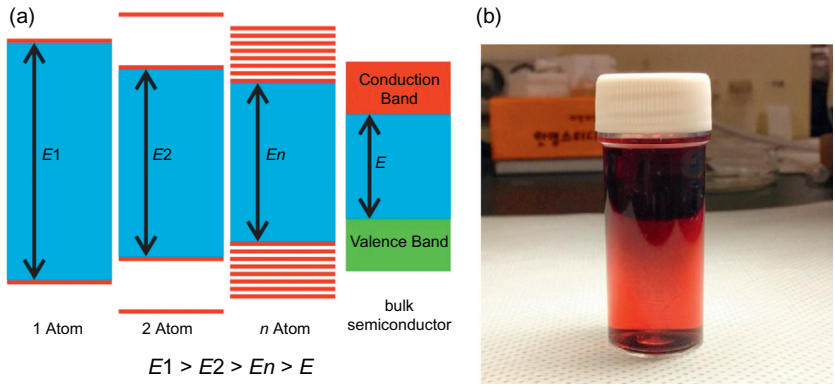

Figure 2.3 (a) Dependence of a quantum-sized semiconductor's band gap on particle size and (b) gold color in the nano form.

$$\text{Its volume } V = \left(\frac{4}{3}\right)\pi r^3 \tag{2.2}$$

$$\text{Surface area to its volume ratio } \frac{A}{V} = \frac{3}{r} \tag{2.3}$$

2.2.2 Quantum Confinement Effect

Contemporary literature on ultradisperse semiconductors distinguishes between the effects arising as a result of increase in surface area and the degree of surface imperfection with decrease in the size of the crystals and, separately, quantum size effects due to radical change in the electronic state of the semiconductor (Figure 2.3a) crystals less than a certain "critical" size, determined in turn by the extent to which the electron–hole pair photogenerated in the semiconductor

is delocalized [5]. These effects also differ in the range of sizes in which they appear. Size effects are observed in semiconductor crystals measuring 10−100 nm, whereas quantum size effects are usually characteristic of nanocrystallites measuring less than 10 nm. In the literature semiconductor nanoparticles in which quantum size effects of one type or another appear, are often called quantum size particles or quantum points to emphasize their special electronic structure. It is necessary to mention the tentative nature of the classification in so far as the exact "critical" size after which the appearance of quantum size effects can be expected is largely determined by the chemical nature of the semiconductor and can vary from 0.5 (CuCl) to 46 (PbSe) or more nanometers. From the positions of quantum mechanics the "critical" size (the threshold for the appearance of quantum size effects) corresponds to the De Broglie wavelength of the free electron. During analysis of the interband absorption of the semiconductor nanoparticle the Bohr radius of the exciton (a_B), which can be calculated from the electrophysical constants of the bulk semiconductor, can be used as such a criterion [6]. The data that have accumulated on size effects in semiconductor nanoparticles make it possible to examine them according to the nature of the effect on the properties of the nanocrystals.

Restriction of the free motion of the exciton in the bulk of the nanocrystal leads to an increase of its energy (E_g^{nano}) in relation to the volume (bulk) semiconductor (E_g^{bulk}). The increase of the energy of the exciton as a result of the quantum size effect ($\Delta E = E_g^{\text{nano}} - E_g^{\text{bulk}}$) can be calculated in the approximation of effective masses, which is based on assumptions about the parabolic nature of the permitted energy bands close to their edges and the invariability of the effective masses of the electron of the conduction band (m_e^*) and the hole of the valence band (m_h^*) in the transition from the bulk to the ultradisperse semiconductors. This approximation gives the following expression for ΔE [7],

$$\Delta E = \frac{\pi^2 \hbar^2}{2R^2}\left(\frac{1}{m_e^*} + \frac{1}{m_h^*}\right) - \frac{1.786e^2}{\varepsilon R} - 0.248R_y^* \tag{2.4}$$

The first term in Eq. (2.4) depends on R^2 and corresponds to the increase in the energy of the exciton as a result of its spatial restriction in the potential box—the semiconductor nanocrystal. The second term determines the energy of columbic interaction of the electron and the hole in the composition of the exciton and increases with decrease in the size of

the nanoparticle. The value of R_y^* in the third term is called the Rydberg energy of the exciton and takes account of the correlation between the motion of the electron and the hole. As seen, the last two terms in Eq. (2.4) lead to a decrease in the energy of the exciton, which is restricted in the volume of the particle. Conventionally, it is known that the color of gold is golden, but at the nanoscale it starts to change dramatically due to quantum size effect. It is found that the colloidal solution of gold nanoparticles is no longer golden but ruby-red in color (Figure 2.3b).

A thin film of gold deposit absorbs across most of the visible part of the electromagnetic spectrum and very strongly in the IR and at all longer wavelengths. It dips slightly around 400−500 nm, and when held up to the light, such a thin film appears blue due to the weak transmission of light in this wavelength range [8]. However, the dilute gold colloid film displays total transparency at low photon energies (below 1.8 eV). Its absorption becomes intense in a sharp band around 2.3 eV (520 nm). This kind of effect is known as surface plasmon, which is aroused from small size of metal particles [9]. Besides quantum size effects, the NsM behavior is different due to surface effects, which dominate as nanocrystal size decreases. Reducing the size of a crystal from 30 to 3 nm, the number of atoms on its surface increases from 5% to 50% beginning to perturb the periodicity of the "infinite" lattice. In that sense, atoms at the surface have fewer direct neighbors than atoms in the bulk and as a result they are less stabilized than bulk atoms. The origin of the quantum size effects strongly depends on the type of bonding in the crystal [10].

In the NsM at least, one dimension being reduced to nanoscale the electronic wavevectors becomes quantized and the system exhibits discrete energy levels. The relevant length scale is the de Broglie wavelength, λ_{dB}, of an electron in one particular direction: If the dimension of the system in one dimension is lower than λ_{dB} we call it a two-dimensional (2D) system. Graphene sheet obtained from exfoliation of graphite is the best example of a 2D system as well as semiconductor superlattices. One-dimensional (1D) system is obtained when two dimensions are lower than λ_{dB} values; nanowires and nanotubes belong to this category [11]. Special is the case of the so-called quantum dots whose all three dimensions are lower than λ_{dB} and we name these as 0D systems. Their energy spectra are discrete and the system can be viewed as an artificial atom. This has a tremendous effect on optical properties of nanoparticles, as the absorption shifts from the

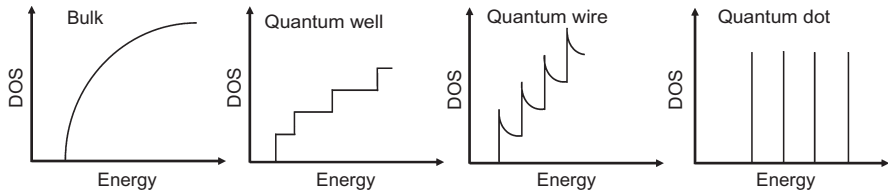

Figure 2.4 Density of states DOS for bulk semiconductor and quantum wells, quantum wires, and quantum dots, respectively.

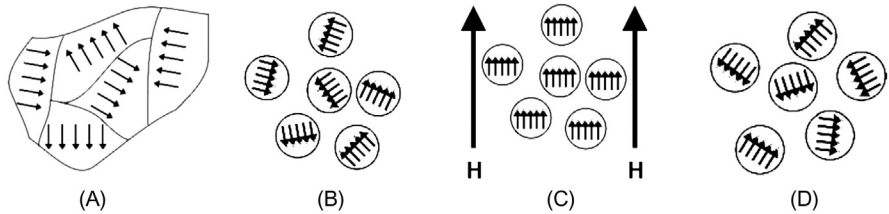

Figure 2.5 Explanation of the superparamagnetic effect.

infrared to the visible range. Quantum confinement in quantum wells (1D), quantum wires (2D), and quantum dots (3D) and the resulting changes of the energy spectrum as shown in Figure 2.4 has also serious implications for the optoelectronic properties of nanostructured semiconductors, and is currently utilized in optoelectronic devices.

2.2.3 Magnetic Effects

Ferromagnetic materials exhibit domains with parallel magnetization (Figure 2.5a). If a magnetic field H is applied, the magnetization of all domains takes the direction of the field and remains in this direction even if the outside field is removed. If the size of ferromagnetic nanoparticles becomes smaller than the critical domain size (10−20 nm), only one domain remains in the particle (Figure 2.5b). If again a magnetic field is applied, all particles will align according to this field (Figure 2.5c), but if the field is removed, thermal motion will lead to a loss of orientation (Figure 2.5d). This behavior is similar to that of permanent magnetic dipoles in a paramagnet and is thus called superparamagnetism [12]. This effect sets, among others, an upper limit to the miniaturization of magnetic memories. On the other hand, superparamagnetic particles are envisioned to play an important role in nanobiotechnology and medicine. Another magnetic nanoeffect, which is used presently in magnetic memories, is the so-called giant magnetoresistive

effect [13]. Depending on the details of the realization, the critical length is either the electron mean free path or the spin relaxation length.

2.3 IMPROVED PERFORMANCE WITH NANOSTRUCTURED PHOTOCATALYSTS

Various facile and cost-effective routes have been investigated and used to design, produce, and characterize numerous NsM, including nanoparticles, nanocubes, nanorods, nanowires, and nanotubes, which maintain fundamentally interesting size-dependent chemical, physical, optical, and many other properties. From the perspective of applications, these structures have wide-ranging utility in areas as diverse as catalysis, energy storage, fiber engineering, fuel cells, biomedicine, computation, power generation, photonics, pollution remediation, and gas sensing. There are few basic parameters, such as synthesis cost, use of nontoxic chemicals, maximum use of aqueous solvents, minimum number of reagents and few steps with high yield, room or low temperature and high efficiency, which needs to be considered during fabrication of advanced devices based on NsM. Nowadays synthesis of new NsM using chemical methods have focused greatly because of low temperature and cost with better functions for environmental and energy applications. The synthesis of NsM is an interesting research field. Until now, a large number of approaches have been explored to synthesize NsM, which could be divided into two major sections, that is, top-down and bottom-up. Interestingly, bottom-up route based on chemistry have attracted considerable attention because of relatively low cost and high yield [14]. In this process, material growth started from atom to atom, molecule by molecule. Recently, a number of techniques, including coprecipitation, sol−gel processes, microemulsions, freeze drying, hydrothermal processes, laser pyrolysis, ultrasound and microwave irradiation, templates, and chemical vapor deposition, have been developed to control the growth, size, morphology, and uniformity of NsM [15]. Therefore, in this section, we will study in brief about heterogeneous photocatalysts fabricated using selective bottom-up approaches for improved photocatalytic activity.

(i) Shortened carrier collection pathways: Photoexcitation produces charge carriers with finite mobility and lifetime, depending on the material, the carrier type, and the light intensity. To drive water redox reactions, these carriers need to reach the material interfaces at the

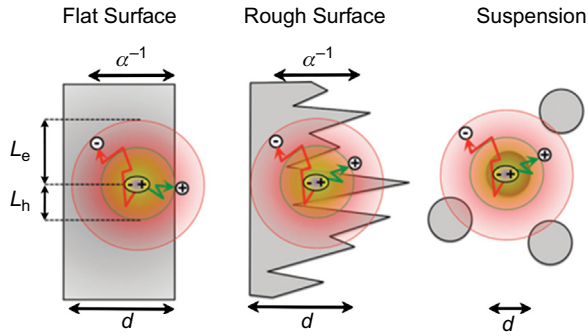

Figure 2.6 Charge collection in flat and nanostructured films and in particle suspensions: d, *film or particle thickness;* L_e, *electron diffusion length;* L_h, *hole diffusion length.*

electrolyte and at the back contact. In the absence of an external field, charge carriers move by diffusion and their range is defined by the mean free diffusion length L. The parameter L depends on the carrier diffusion constant D and the carrier lifetime τ (Eq. (2.5)), and a dimensionality factor ($q = 2, 4, 6$ for 1, 2, or 3D diffusion).

$$\overline{L}^2 = qD\tau \tag{2.5}$$

For intrinsic semiconductors, usually $L_e > L_h$ because of the larger diffusion constant D of the electrons compared to holes. Upon doping NsM, the concentration of the majority carriers increases, and with it their τ and L values. On the contrary, the lifetime and diffusion length of the minority carriers decrease [16]. For optimum collection of both carrier types at the back contact, the semiconductor film thickness d has to be in the same range as L_e and L_h (Figure 2.6). To improve minority carrier collection at the semiconductor–electrolyte interface, the surface roughness of the film can be increased. This surface nanostructuring approach is particularly useful for first row transition metal oxides (MnO_2, Fe_2O_3), which suffer from low hole mobility and lifetimes [17]. Ideal electron/hole collection is possible with suspended nanoparticles, if their particle size $d < L_e$, L_p. Although in this situation, both carrier types need to be extracted at the sc–electrolyte interface. Thus, there is a need for selective redox agents. This has been referred to by Helmut Tributsch as kinetic rectification [18].

(ii) Improved light distribution: The ability of a material to absorb light is determined by the Lambert–Beer law and the wavelength-dependent absorption coefficient α. The light penetration depth α^{-1}

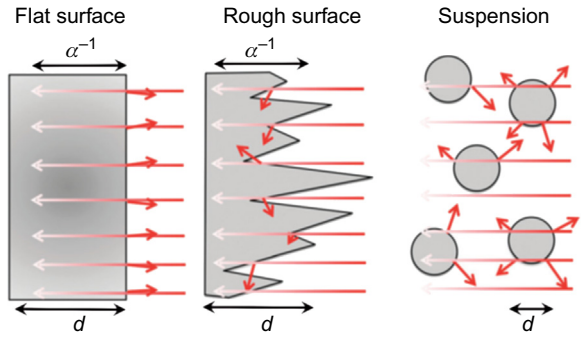

Figure 2.7 Light distribution in flat and nanostructured films, and in particle suspensions: d, *film or particle thickness.*

refers to the distance after which the light intensity is reduced to 1/*e* of the original value. For example, for Fe_2O_3, $\alpha^{-1} = 118$ nm at $\lambda = 550$ nm, for CdTe, $\alpha^{-1} = 106$ nm (550 nm), and for Si, $\alpha^{-1} = 680$ nm (510 nm) [19]. To ensure >90% absorption of the incident light, the film thickness must be >2.3 times the value of α^{-1} (Figure 2.7). Surface-structuring on the micro- or nanoscale can increase the degree of horizontal light distribution by light scattering. This "trapped" light would otherwise be lost by direct reflection from a flat surface [20]. Light scattering is maximal in particle suspensions, because it can occur at both the front and back sides of the particles.

(iii) Surface area-enhanced charge transfer: The larger specific surface area of nanomaterials promotes charge transfer across the material interfaces (solid−solid and solid−liquid), allowing water redox reactions to occur at relatively low current densities and, correspondingly, low over potentials. In other words, the increase of surface area allows to better match the photocurrents with the slow kinetics of the water redox reactions [21]. In particular proceed at Fe_2O_3 and TiO_2, according to recent transient absorption measurements. Thus, increases of surface area reduce the need for highly active, and often expensive, cocatalysts, based on Ir, Rh, or Pt [22].

(iv) Multiple exciton generation: The altered electronic structure of strongly size-confined nanocrystals gives rise to multiple exciton generation (MEG), that is, the formation of several (*n*) electron−hole pairs after absorption of one photon with an energy *n* times the band gap of the dot (Figure 2.8). The MEG effect is responsible for the abnormally high efficiency of PbSe QD-sensitized TiO_2 PEC cells, and PbSe

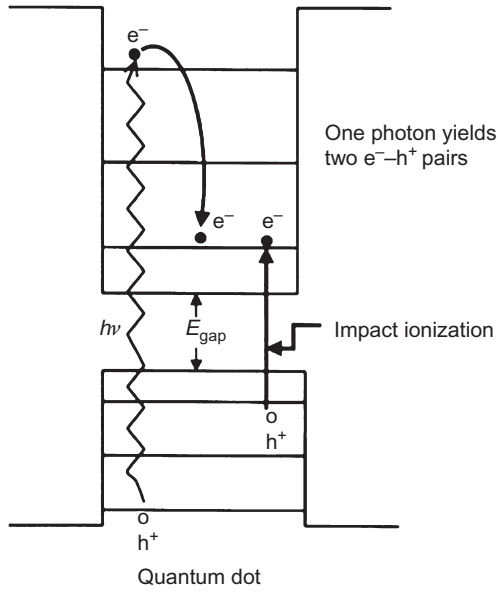

Figure 2.8 Enhanced photovoltaic efficiency in QD solar cells by impact ionization.

photovoltaic cells [23]. The effect has not yet been applied to water photoelectrolysis. Future MEG-enhanced water splitting devices will likely be Tandem or multi-junction devices, because the individual quantum dots cannot produce a sufficient potential for overall water splitting. This is because for efficient solar energy conversion, the band gaps of the relevant dots need to be a fraction of the energy of visible light photons ($E = 1.55-3.1$ eV).

2.4 APPLICATIONS OF NANOSTRUCTURED PHOTOCATALYSTS

Both the technological and economic importance of photocatalysis have increased considerably over the past decade. Improvements in performance have been strongly correlated to advances in nanotechnology; for example, the introduction of nanoparticulate photocatalysts has tremendously enhanced the catalytic efficiency of specific materials. A variety of applications ranging from anti-fogging, antimicrobial, and self-cleaning surfaces, through to water and air purification and solar-induced hydrogen production, have been developed and many of these have made their way into commercial products. However, extensive research continues to further optimize this

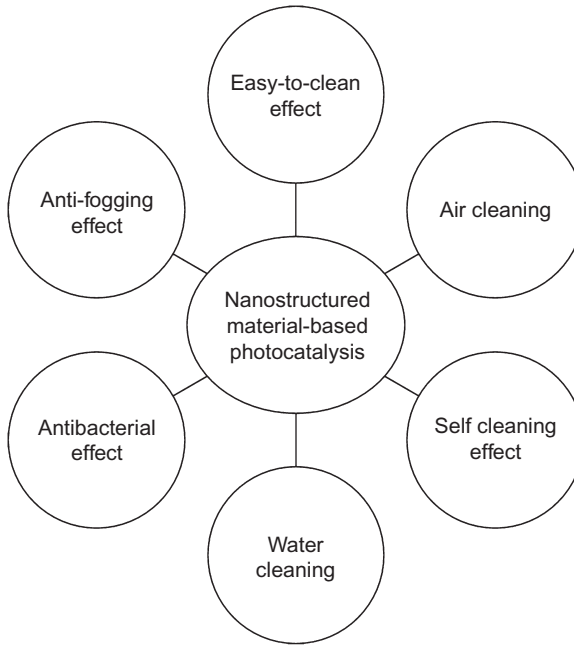

Figure 2.9 Photocatalysis applications.

technology and to widen the spectrum of potential applications. Research and application foci include anti-stick or anti-fingerprint coatings, soil repellency, and decomposition of organic matter, such as microbes or fat. When exposed to light certain semiconducting materials such as "photocatalysts" trigger or accelerate chemical reactions resulting, for example, in a decomposition of organic molecules [24]. Due to their large surface area, nanosized catalyst particles show a significantly enhanced reactivity compared to larger particles or bulk material. Numerous materials are under examination; however, none appear to match the efficiency of TiO_2. Its application requires illumination in the UV or at the extreme blue edge of the visible spectrum. Volume applications are thus mainly limited to the outdoor area [25]. However, despite the reduced natural illumination, even indoor products such as sanitary ceramics are being increasingly applied. Moreover, research is underway to widen the exploitable spectral range toward visible light. A few applications of photocatalysis are provided in Figure 2.9. In recent years, applications have been directed toward environmental clean-up, drinking water treatment, industrial, and health applications.

(i) Removing trace metals: Trace metals, such as mercury (Hg), chromium (Cr), lead (Pb), and other metals, are considered to be highly hazardous to health. Thus, removing these toxic metals is essentially important for human health and water quality. The environmental applications of heterogeneous photocatalysis include removing heavy metals such as mercury (Hg), chromium (Cr), cadmium (Cd), lead (Pb), arsenic (As), nickel (Ni), and copper (Cu). The photoreducing ability of photocatalysis has been used to recover expensive metals from industrial effluent, such as gold, platinum, and silver [26].

(ii) Destruction of organics: Photocatalysis has been used for the destruction of organic compounds, such as alcohols, carboxylic acids, phenolic derivatives, or chlorinated aromatics, into harmless products, for example, carbon dioxide, water, and simple mineral acids. Water contaminated by oil can be treated efficiently by photocatalytic reaction. Herbicides and pesticides that may contaminate water, such as 2,4,5-trichlorophenoxyacetic acid, 2,4,5-trichlorophenol, and s-triazine herbicides, can be also mineralized [27].

(iii) Removing inorganic compounds: In addition to organic compounds, wide ranges of inorganic compounds are sensitive to photochemical transformation on the catalyst surfaces. Inorganic species such as bromate, or chlorate, azide, halide ions, nitric oxide, palladium and rhodium species, and sulfur species can be decomposed [28]. Metal salts such as $AgNO_3$, HgCl, and organometallic compounds (e.g., CH_3HgCl) can be removed from water, as well as cyanide, thiocyanate, ammonia, nitrates, and nitrites.

(iv) Water disinfections: Photocatalysis can also be used to destroy bacteria and viruses. *Streptococcus mutans*, *Streptococcus natuss*, *Streptococcus cricetus*, *Escherichia coli*, *Saccharomyces cerevisiae*, *Lactobacillus acidophilus*, and poliovirus 1 were destructed effectively using heterogeneous photocatalysis [29]. The increasing incidence of algal blooms in fresh water supplies and the consequent possibility of cyanobacterial microcystin contamination of potable water microcystin toxins is also degraded on immobilized titanium dioxide catalyst. Photodisinfection sensitized by TiO_2 had some effect on the degradation of *Chlorella vulgaris* (Green algae), which has a thick cell wall.

(v) Degradation of natural organic matter: Humic substances (HS) are ubiquitous and defined as a category of naturally occurring biogenic

heterogeneous organic substances that can be generally characterized as being yellow-brown and having high molecular weights [30]. These are also defined as the fraction of filtered water that adsorb on XAD-8 resin (nonionic polymeric adsorbent) at pH 2. They are the main constituents of the dissolved organic carbon pool in surface waters (freshwaters and marine waters), and ground waters, commonly imparting a yellowish-brown color to the water system. The concentration of HS varies from place to place; the values in seawater being normally from 2 to 3 mg L^{-1}. Their size, molecular weight, elemental composition, structure, and number and position of functional groups vary, depending on the origin and age of the material. HS are known to affect the behavior of some pollutants significantly in natural environments, such as trace metal speciation and toxicity, solubilization and adsorption of hydrophobic pollutants, and aqueous photochemistry. HS act as substrates for bacterial growth, inhibit the bacterial degradation of impurities (some color) in natural water, and form complex with heavy metals such as Fe, Pb, and Mn making it harder to remove them, transport the metals in the environment, and also promote the corrosion of pipes. HSs act as a source of methyl groups and thus react with hypochlorite ion, which is used as a biocide in water treatment plants, to produce disinfectant byproducts, for example, trihalomethanes, haloacetic acids, other chlorinated compounds, and nitriles, some of which are suspected to be carcinogenic. More than 150 products have been identified when HS react with chlorine [31]. Recently, 3-chloro-4-(dichloromethyl)-5-hydroxy-2(5H)-furanone [abbreviated as (MX)] was found in the chlorinated water containing HS. Advanced oxidation has been applied to decreasing the organic content in water including humic acid. It has the advantage of not leaving any toxic byproducts or sludge [32]. Heterogeneous photocatalysis was also coupled with other physical methods to increase the degradation rate of organic molecules including HA (sono-photocatalysis, ozonation photocatalysis).

(vi) Seawater treatment: Recently, HS was also decomposed in highly saline water (artificial seawater) and natural seawater using different photocatalytic materials. The decomposition rate of HS in seawater was slow compared with pure water media. No toxic byproducts were detected during the decomposition. Minero et al. [33] studied the decomposition of some components in crude oil (dodecane and toluene) in the seawater media. They found that no chlorinated compounds have been detected during the irradiation, and complete

decomposition was achieved after a few hours of irradiation. Another study conducted on the decomposition of seawater-soluble crude oil fractions found that it can be decomposed under illumination of nanoparticles of TiO_2 using artificial light.

(vii) Air cleaning: The photocatalytic process is well recognized for the removal of organic pollutants in the gaseous phase, such as volatile organic compounds, having great potential applications to contaminant control in indoor environments, such as residences, office buildings, factories, aircraft, and spacecraft. To increase the scope of the photocatalytic process in the application to indoor air, the disinfection capabilities of this technique are under investigation. Disinfection is of importance in indoor air applications because of the risk of exposure to harmful airborne contaminants. Bioaerosols are a major contributor to indoor air pollution, and more than 60 bacteria, viruses, and fungi have been documented as infectious airborne pathogens. Diseases transmitted through bioaerosols include tuberculosis, legionaries, influenza, colds, mumps, measles, rubella, small pox, aspergillosis, pneumonia, meningitis, diphtheria, and scarlet fever [34]. Traditional technologies to clean indoor air include the use of activated charcoal filters, HEPA filters, ozonation, air ionization, and bioguard filters. None of these technologies is completely effective.

Photocatalytic oxidation can also inactivate infectious microorganisms, which can be airborne bioterrorism weapons, such as *Bacillus anthracis* (anthrax). A photocatalytic system was investigated by Knight in 2003 to reduce the spread of severe acute respiratory syndrome on flights, following the outbreak of the disease. Similarly, in 2007 the avian influenza virus A/H5N2 was shown to be inactivated from the gaseous phase using a photocatalytic prototype system [35]. Inactivation of various Gram-positive and Gram-negative bacteria using visible light and a doped catalyst and fluorescent light irradiation similar to that used in indoor environments was studied and shows great promise for widespread applications. It was also shown that *E. coli* could be completely mineralized on a coated surface in air. Carbon mass balance and kinetic data for complete oxidation of *E. coli*, *Aspergillus niger*, *Micrococcus luteus*, and *Bacillus subtillus* cells and spores were subsequently presented. A comprehensive mechanism and detailed description of the photokilling of *E. coli* on coated surfaces in air has been extensively studied in order to understand to a considerable degree and in a quantitative way the kinetics of *E. coli*

immobilization and abatement by photocatalysis, using FTIR, AFM, and CFU as a function of time and peroxidation of the membrane cell walls. Novel photoreactors and photo-assisted catalytic systems for air disinfection applications such as those using polyester supports for the catalyst, carbon nanotubes, combination with other disinfection systems, membrane systems, use of silver bactericidal agents in cotton textiles for the abatement of *E. coli* in air, high surface area CuO catalysts, and structure silica surfaces have also been reported. In terms of environmental health, the antifungal capability of photocatalysis against mold fungi on coated wood boards used in buildings was confirmed using *A. niger* as a test microbe, and UVA irradiation [36].

2.5 CONCLUSION

The photocatalytic technique is a versatile and efficient disinfection process capable of inactivating a wide range of harmful microorganisms in various media. It is a safe, nontoxic, and relatively inexpensive disinfection method whose adaptability allows it to be used for many purposes. Research in the field of photocatalytic disinfection is very diverse, covering a broad range of applications. Particularly, the use of photocatalysis based on NsM was shown to be effective for various air-cleaning applications to inactivate harmful airborne microbial pathogens, or to combat airborne bioterror threats, such as anthrax. Photocatalytic thin films on various substrates were also shown to have a potential application for "self-disinfecting" surfaces and materials, which can be used for medical implants, "self-disinfecting" surgical tools, and surfaces in laboratory and hospital settings, and equipment in the pharmaceutical and food industries. Photocatalytic food packaging was shown to be a potential way to reduce the risk of foodborne illnesses in cut lettuce and other packaged foods. In terms of plant protection, photocatalysis is being investigated for use in hydroponic agricultures as an alternative to harsh pesticides. For water treatment applications, photocatalytic disinfection has been studied and implemented for drinking water production using novel reactors and solar irradiation. Eutrophic waters containing algal blooms were also shown to be effectively treated using coated hollow beads and solar irradiation. The effectiveness of photocatalytic disinfection for inactivating microorganisms of concern for each of these applications was presented, highlighting key studies and research efforts conducted. While the performance of this technology is still to be optimized for the

specific applications, based on the literature presented, it is abundantly evident that photocatalysis should be considered a viable alternative to traditional disinfection methods in some cases.

In a move toward a more environmentally friendly world, traditional solutions to classic problems, such as the production of safe drinking water, must shift toward more sustainable alternatives. Photocatalytic disinfection is not only a replacement technology for traditional methods in traditional applications, but also a novel approach for solving other disinfection problems, such as the control of bioterror threats. In this sense, the strength of photocatalytic disinfection lies in its versatility for use in many different applications.

REFERENCES

[1] Siegel RW. Nanostructured materials—mind over matter. Nanostruct Mater 1993;3:1–18.

[2] Hu X, Li G, Yu JC. Design, fabrication, and modification of nanostructured semiconductor materials for environmental and energy applications. Langmuir 2010;26:3031–9.

[3] Gleiter H. Nanostructured materials: basic concepts and microstructure. Acta Mater 2000;48:1–29.

[4] Koch CC. Synthesis of nanostructured materials by mechanical milling: problems and opportunities. Nanostruct Mater 1997;9:13–22.

[5] Obare SO, Meyer GJ. Nanostructured materials for environmental remediation of organic contaminants in water. J Environ Sci Health Part A 2004;A39:2549–82.

[6] Alivisatos AP. Semiconductor clusters, nanocrystals, and quantum dots. Science 1996;217:933–7.

[7] Brus LE. Electron-electron and electron-hole interactions in small semiconductor crystallites—the size dependence of the lowest excited electronic state. J Chem Phys 1984;80:4403–9.

[8] Moriarty P. Nanostructured materials. Rep Prog Phys 2001;64:297–381.

[9] Oelhafen P, Schuler A. Nanostructured materials for solar energy conversion. Solar Energy 2005;79:110–21.

[10] Logothetidis S. Nanostructured materials and their applications. Springer; 2011. p. 6.

[11] Davies AG, Thompson JMT. Advances in nanoengineering electronics, materials and assembly. Royal Society Series on Advances in Science, vol. 3. London: Imperial College Press; 2007. p. 3.

[12] Reithmaier JP, Petkov P, Kulisch W, Popov C. Nanostructured materials for advanced technological applications. Springer; 2009. p. 6.

[13] Anderson JC, Leaver KD, Rawlings RD, Alexander JM. Materials Science, London: Chapman & Hall; 1990.

[14] Gleiter H. Materials with ultrafine microstructures: petrospectives and perspectives. Nanoscruct Mater 1992;1:1–19.

[15] Osterloh FE. Inorganic nanostructures for photoelectrochemical and photocatalytic water splitting. Chem Soc Rev 2013;42:2294–320.

[16] Berger LI. In: Lide DR, editor. CRC handbook of chemistry and physics, vol. 88. Boca Raton, FL: CRC Press/Taylor and Francis; 2008.

[17] Emary C. Theory of nanostructures. 2009, p. 26 [Chapter 1].

[18] Tributsch H. Photovoltaic hydrogen generation. Int J Hydrogen Energy 2008;33:5911–30.

[19] Wang Z, Liu Y, Huang B, Dai Y, Lou Z, Wang G, et al. Progress on extending the light absorption spectra of photocatalysts. Phys Chem Chem Phys 2014;16:2758–74.

[20] Polman A, Atwater HA. Photonic design principles for ultrahigh-efficiency photovoltaics. Nat Mater 2012;11:174–7.

[21] Cowan AJ, Tang JW, Leng WH, Durrant JR, Klug DR. Water splitting by nanocrystalline TiO_2 in a complete photoelectrochemical cell exhibits efficiencies limited by charge recombination. J Phys Chem C 2010;114:4208–14.

[22] Tang JW, Durrant JR, Klug DR. Mechanism of photocatalytic water splitting in TiO_2. Reaction of water with photoholes, importance of charge carrier dynamics, and evidence for four-hole chemistry. J Am Chem Soc 2008;130:13885–91.

[23] Semonin OE, Luther JM, Choi S, Chen HY, Gao JB, Nozik AJ, et al. Nanocrystal solar cells squeeze extra juice out of sunlight. Science 2011;334:1530–3.

[24] Hashimoto K, Irie H, Fujishima A. TiO_2 photocatalysis: a historical overview and future propsects. Jpn J Appl Phys 2005;44:8269–85.

[25] Nakat K, Fujishima A. TiO_2 photocatalysis: design and applications. J Photochem Photobio C: Photochem Rev 2012;13:169–89.

[26] Nakata K, Ochiai T, Murakami T, Fujishima A. Photoenergy conversion with TiO_2 photocatalysis: new materials and recent applications. Electrochem Acta 2012;84:103–11.

[27] Gamage J, Zhang Z. Applications of photocatalytic disinfection. Int J Photoenergy 2010;2010:1–12.

[28] Blake DM, Maness PC, Huang Z, Wolfrum EJ, Huang J, Jacoby WA. Application of the photocatalytic chemistry of titanium dioxide to disinfection and the killing of cancer cells. Separ Purif Methods 1999;28:1–50.

[29] Ljubas D. Solar photocatalysis-a possible step in drinking water treatment. Energy 2005;30:1699–710.

[30] Basca R, Kiwi J, Ohno T, Albers P, Nadtochenko V. Preparation, testing and characterization of doped TiO_2 able to transform biomolecules under visible light irradiation by peroxidation/oxidation. J Phys Chem B 2005;109:5994–6003.

[31] Kern P, Schwaller P, Michler J. Electrolytic deposition of titania films as interference coatings on biomedical implants: microstructure, chemistry and nano-mechanical properties. Thin Solid Films 2006;494:279–86.

[32] Walther BA, Ewald PW. Pathogen survival in the external environment and the evolution of virulence. Bio Rev Camb Philos Soc 2004;79:849–69.

[33] Minero C, Maurino V, Pelizzetti E. Photocatalytic transformations of hydrocarbons at the sea water/air interface under solar radiation. Marine Chem 1997;58:361–72.

[34] Goswami DY, Vijayaraghavan S, Lu S, Tamm G. New and emerging developments in solar energy. Solar Energy 2004;76:33–43.

[35] Jacoby WA, Maness PC, Wolfrum EJ, Blake DM, Fennell JA. Mineralization of bacterial cell mass on a photocatalytic surface in air. Environ Sci Technol 1998;32:2650–3.

[36] Chen F, Yang X, Wu Q. Antifungal capability of TiO_2 coated film on moist wood. Build Environ 2009;44:1088–93.